Effect of Sintering Atmosphere on the Shear Properties of Pressureless Sintered Silver Joint

S.T. Chua, K.S. Siow[1, 2] and A.Jalar
Institute of Microengineering and Nanoelectronics (IMEN),
Universiti Kebangsaan Malaysia,
43600 Bangi, Selangor, Malaysia.
Email: kimsiow@ukm.edu.my[1]; kimshyong@gmail.com[2]

Abstract

Sintered silver is a possible replacement for high performance and Pb free die attach materials in power modules and traditional microelectronic packages because of its high melting temperature, high thermal conductivity and good thermo-mechanical properties. However, reliable sintered silver joints can only be easily formed on Ag or Au plated surfaces during pressure sintering. Here we present the initial results of two pressure-less Ag pastes (i.e. micron-sized flakes and nanoparticles) that can sinter on copper (Cu). These sintered Ag joints exceeded the minimum die shear strength as per MIL-STD883E; nano-Ag preferred the N_2-5%H_2 environment to produce die shear strength of 17 MPa on the H_2 cleaned Cu while micron-Ag joint produced die shear strength of 14 MPa on the Cu substrate when sintered in ambient air. Fractography of sintered nano-Ag joints showed that the silver particles have necked to different degrees in N_2 and N_2-5%H_2. Heavy oxidation caused by ambient air sintering prevented bonding of nano-Ag on the Cu oxide, resulting in a flat fratography. Similar flat fractograph was also visible for micron-Ag sintered in N_2 atmosphere because of residual binders prevented the sintering on the Cu substrate. In the presence of ambient air, the oxidative combustion of the binders and capping agents de-oxidized the Cu substrate to allow sintering onto the Cu. Cross section of this micron-Ag joint on Cu substrate confirmed the joint formation in ambient air during pressureless sintering. These results showed that different binders and capping agents influence the sintering properties differently to produce reliable sintered Ag joints.

Keywords – **low-temperature sintering, lead-free die attach, sintered silver, nano-silver.**

1.0 Introduction

Die attach materials are one of the few remaining materials in the microelectronic packaging yet to migrate to more environmental friendly product. The delay is caused by lack of available suitable replacements that are reliable and cost-effective[1]. In the power module sector, the advent of SiC and GaN necessitate the use of die attach materials with thermal performance and reliability better than current Pb-Sn or Sn-Ag-Cu and Sn-Ag solder [2]. Sintered silver emerges as one of the potential candidates because of its relatively low processing temperature, high melting temperature, high thermal conductivity and thermo-mechanical reliability [3, 4].

However, most commercially available silver paste can only form reliable sintered Ag joint on Ag or gold (Au) plated substrate during pressure sintering [5, 6]. Application of pressure during sintering may damage the circuitry on the silicon dies and pose a reliability issue to the devices. Ag or Au-plating on the substrate also adds extra costs to the manufacturers.

Hence, there is a need to develop pressureless sintered silver paste, whether using micron-Ag flakes or nano-Ag particles, to form this die attach joint. In this research, we evaluate two newly developed pressureless silver pastes to determine their thermal events and sintering characteristics during joint formation and the corresponding die shear strength on copper (Cu) substrates.

2.0 Experiment Procedure

2.1 Materials

Micron-sized Ag flakes and Ag nanoparticles pressureless pastes were obtained from suppliers, herein named as micron-Ag and nano-Ag respectively. Typical content of these silver pastes can be referred here [3]. Cu alloy (type: C194 with nominal composition of 97.4%Cu, 2.4%Fe, 0.1%Zn) and silicon of "2.8 mm x 1.8 mm" in size with backmetallization of TiNiAg were used as substrates and dies for this study.

2.2 Sample Preparation

Micron-Ag silver pastes of 75 μm in thickness were printed on the Cu substrate before placing the Si dies and then sintering at 230°C. Similar to micron-Ag paste, the nano-Ag paste was applied to the Cu substrate before an interim drying step of 100°C before placing the silicon die and sintering at peak temperature of 250°C. Three different environments i.e. ambient air, nitrogen (N_2) and forming gas (N_2-5%H_2), were used to sinter the silver pastes.

2.3 Differential Scanning Calorimetry and Thermogravimetric Analysis

TGA NETZSCH TG 209F1 Libra was used to analyze the Ag pastes in ambient air and N_2 while NETZSCH DSC 204F1 Phoenix was used to analyze the Ag paste in air, N_2 and N_2-5%H_2 from room temperature to 350 °C at a heating rate of 10K/min.

2.4 Die Shear test and Fracture surface

The die shear tests were carried out at a rate of 300 μm/sec and other criteria as per MIL-STD 883E. After the die-shear test, the fracture surfaces were observed under SEM Hitachi S3400 and EDX (X-Max Horiba 50mm^2).

3.0 Results and Discussions

3.1 TGA of micron-Ag and nano-Ag pastes

The TGA curves, in Fig. 1, show that the micron-Ag pastes lose 12% of weight while nano-Ag pastes lose 13-14% of their weights in air or N_2 environment during these thermal excursions. Derivatives of these TGA curves for micron-Ag pastes show the maximum loss occur at 200 °C though onset of the weight loss begins earlier at 192 °C (Fig. 2). In the case of nano-Ag paste, the onset of the weight loss occurred from 165 °C with a maximum loss at 215 °C. These losses were attributed to solvent vaporization and desorption or oxidative combustion of the binders and capping agents in the Ag pastes.

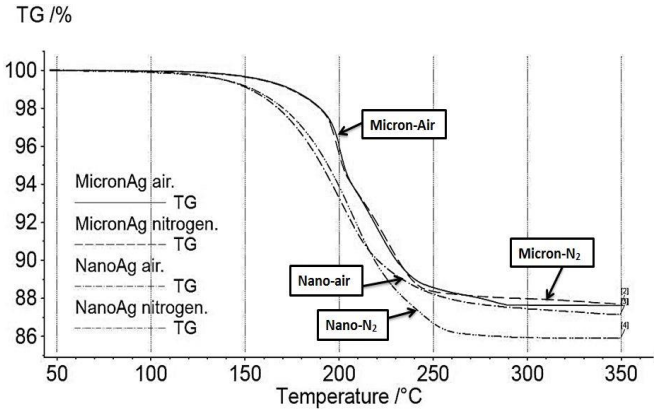

Fig. 1: TGA of micron-Ag and nano-Ag in air and N_2.

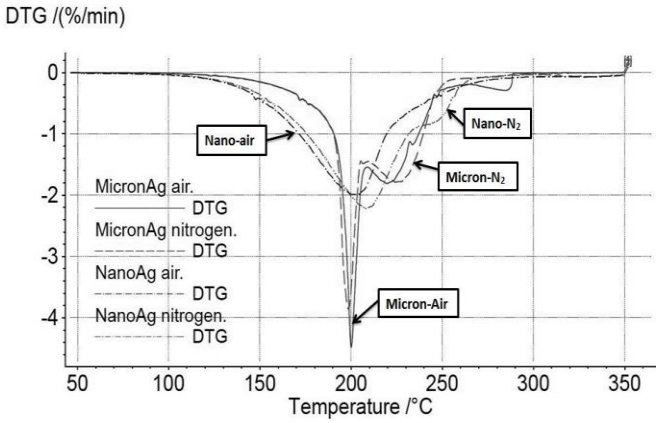

Fig. 2: DTG (of Fig. 1) of micron-Ag and nano-Ag in air and N_2.

3.2 DSC of micron-Ag pastes

As shown in Fig. 3, the DSC thermograms of micron-Ag pastes show a slight endothermic peak at temperature 190°C before a sharp exothermic peak at 200°C in the N_2 and N_2-5%H_2 environment. These peaks coincide with the TGA mass loss, shown in Fig. 1, which also occur at 200 °C. The sharp exothermic peak could be attributed to the sintering activities of the silver pastes and oxidative combustion of the organic binders and agents. Similarly, this micron-Ag paste, in the presence of ambient air, also showed a huge exothermic peak from 200°C till 300°C with multiple peaks at 227°C, 257°C and 289°C.

In the absence of oxygen from ambient air, the micron-Ag paste showed a broad endothermic peak till 280°C in N_2 and N_2-5%H_2. This endothermic peak could be attributed to the decomposition of AgO to Ag_2O or Ag; such reduction had been reported to occur at temperatures ranging from 200°C till 400°C [7-9]. Micron-Ag paste relies on this endothermic silver compound to join neighbouring micron silver flakes. This endothermic reaction could have been masked by the huge exothermic reaction of binder decomposition in the presence of ambient air for the micron-Ag paste. However, these thermal events need to be confirmed by FTIR-DSC chemical analysis of the de-sorbents.

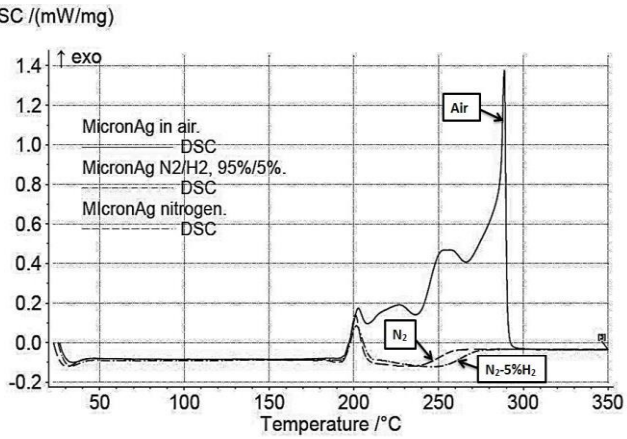

Fig. 3: DSC of micron-Ag paste in air, N_2 and N_2-5%H_2

3.3 DSC of nano-Ag pastes

Fig. 4 shows the absence of discernible exothermic peaks for the DSC analysis of nano-Ag pastes in N_2 and N_2-5%H_2 environment. Both thermograms exhibited broad endothermic peaks from 180°C with peaks appearing at 219°C and 237 °C for N_2-5%H_2 and N_2 respectively. These endotherms corresponded to mass loss reported in the TGA carried out in N_2 (Fig. 2). This correspondence suggested that desorption instead of oxidative combustion of the binder-solvent in the Ag pastes because of the absence of the oxygen in the N_2 and N_2-5%H_2 environment. Such desorption is often reported for sol-gel system [10] but further analysis with DSC-FTIR is needed to confirm our hypothesis. This massive desorption was likely to offset the exothermic peak associated with the sintering of nano-Ag particles.

In ambient air, the DSC analysis of the nano-Ag paste showed exothermic peaks at 276°C and 326°C. The onset of the first exothermic peak at 214°C coincides with the maximum weight reduction in the TGA curve shown in Fig. 2. These exotherms could be attributed to the oxidative reaction of the binders in the nano-Ag paste. There was no loss of mass in TGA curves associated with the highest exothermic peak at 326 °C but some catalytic reactions involving binder and nano silver particles could have caused these exothermic peaks [11].

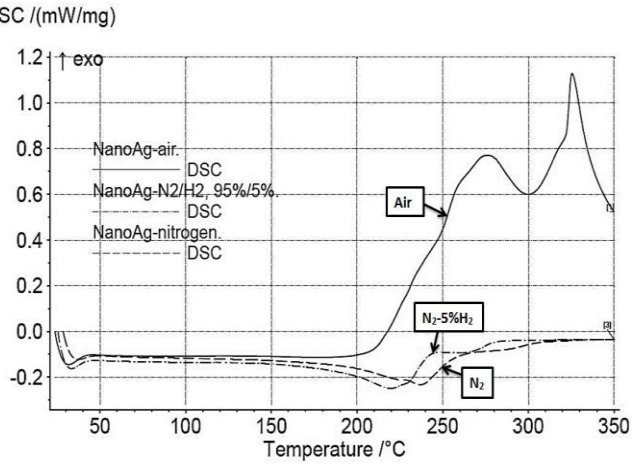

Fig. 4: DSC of nano-Ag paste in air, N_2 and N_2-5%H_2

3.4 Die shear test of micron-Ag joint

Based on Fig. 5, sintering micron-Ag paste in air produce joint of higher strength than that produce in N_2-5%H_2. The oxidative combustion of the binder in air reduced the Cu oxide on the Cu substrate and allowed Ag flakes of micron-Ag paste to sinter directly onto the Cu substrate [12, 13]. This sintering is evident from the cross-section of the sintered micron-Ag joint shown in Fig. 6a. The strong bonds between Ag flakes and the Cu substrate transferred the failure interface to the die attach layers of the sintered Ag joint. The fractured Ag joint, as shown in Fig. 7a and 7b, shows grain coarsening and interparticle necking of neighbouring Ag flakes. Signs of plastic deformation, such as elongated grains, were also visible on the fracture surface of the sintered micron-Ag joint.

In the presence of N_2-5%H_2 environment, the die shear strength reduced significantly to 7 MPa (based on t-test, 95% confidence) and its failure interface shifted to a mixed mode of Ag-Cu interface and die attach layer of the sintered Ag joint. The cross-section of this micron-Ag joint, shown in Fig. 6b, shows good bonding to the Cu substrate as well as back-metallization on the silicon. This interfacial bonding resulted in plastic deformation within the sintered silver albeit without visible necking on the silver flakes (Fig. 7c and 7d).

When sintering was carried out in N_2 atmosphere, the micron-Ag joint did not register any shear strength and all failure occurred at the Cu and sintered Ag joint interfaces. Fig. 7e and 7f show the flat fracture surfaces without any visible signs of sintering. An EDX analysis of similarly sintered micron-Ag paste also confirms the presence of carbon possibly from the binder and capping agent (Fig. 8). As shown in the cross-section of the micron Ag joint (Fig. 6c), this residual binder prevents the sintering of micron-Ag paste on the Cu substrate but does not prevent any self-sintering amongst the micron-Ag flakes.

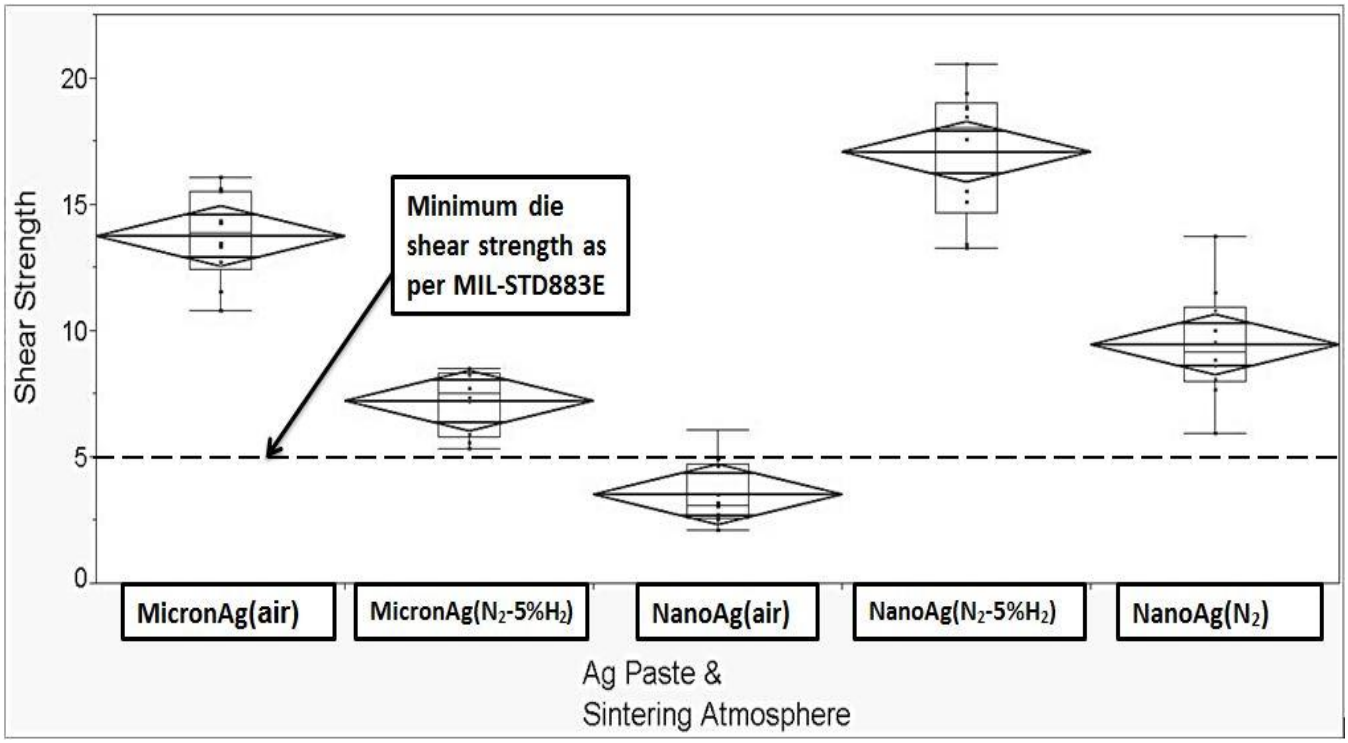

Fig 5: Die shear strength of micron-Ag and nano-Ag paste sintered on Cu substrate in air, N_2, N_2-5%H_2.

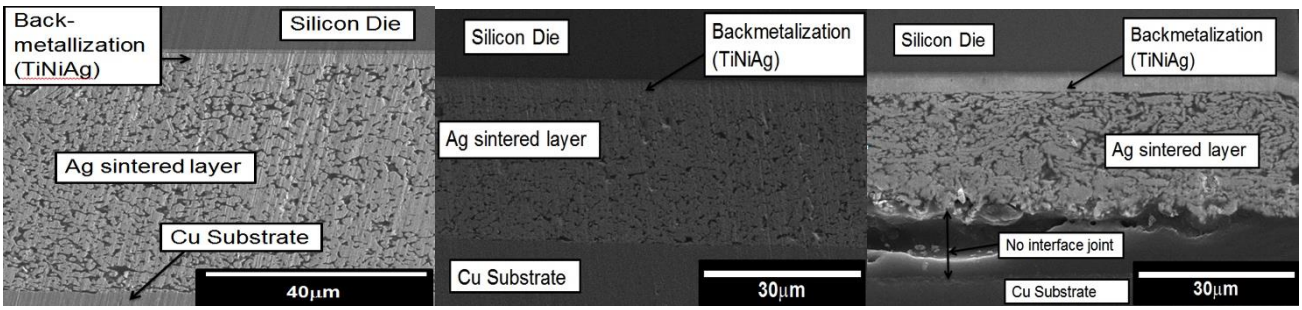

a) Air b) N_2-5%H_2 c) N_2

Fig. 6: Cross-section of micron-Ag joint sintered on Cu substrate under different environment: a) air b) N_2-5%H_2 and c) N_2

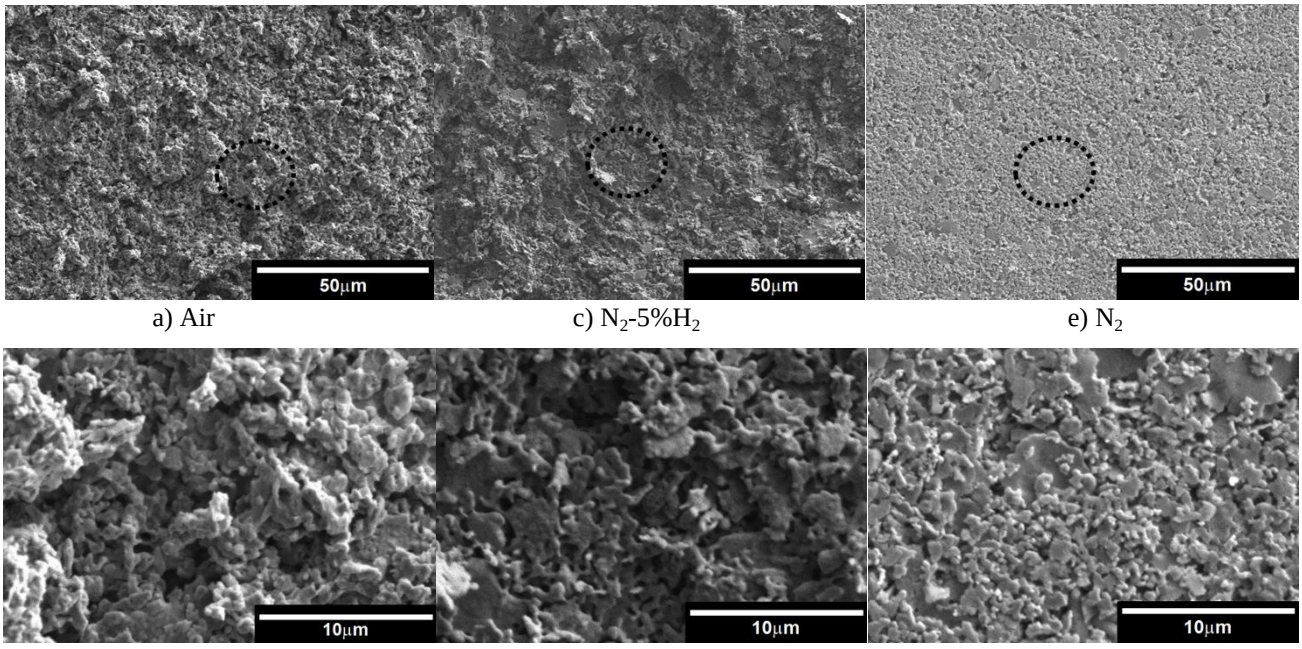

a) Air c) N_2-5%H_2 e) N_2

b) Air d) N_2-5%H_2 f) N_2

Fig. 7: Fracture surface of micron-Ag sintered in different environment

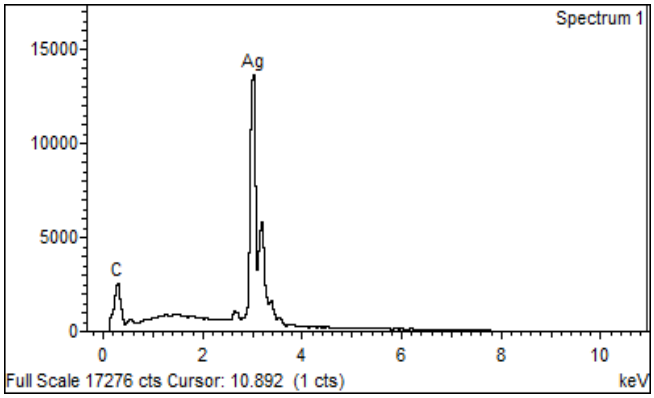

Fig. 8: EDX analysis of micron-Ag sintered in N_2 environment.

3.5 Die shear test of nano-Ag joint

In the case of nano-Ag joint, sintering in N_2-5%H_2 produces the highest shear strength followed by those sintered in N_2 and ambient air (Fig. 5).

Although sintering in ambient air produces huge exothermic reaction as reported in the DSC analysis (Fig. 4), the oxygen also oxidizes the Cu substrate and thus prevents the Ag nanoparticles from sintering onto the Cu substrate. SEM and EDX analysis of the fracture surface on the Cu substrate (Fig. 9a and 9b), clearly supports this conjecture. Residuals carbon was also detected on this surface. Unlike micron-Ag paste, the binders of the nano-Ag paste are insufficient or unsuitable to reduce the Cu oxide to Cu. This condition produced shear strength of only 4 MPa that is less than requirement of MIL-STD 883E. The fracture interface shifts to the Ag-Cu substrate interface and die attach layer of the sintered nano-Ag joint (Fig. 10a and 10b).

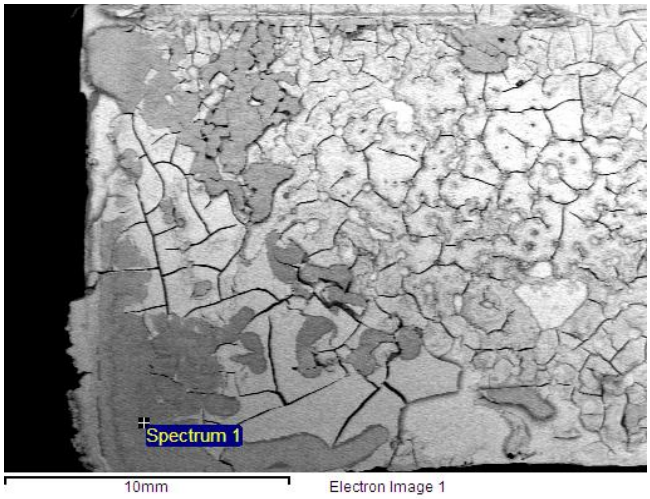

a) SEM image with EDS spot analysis location

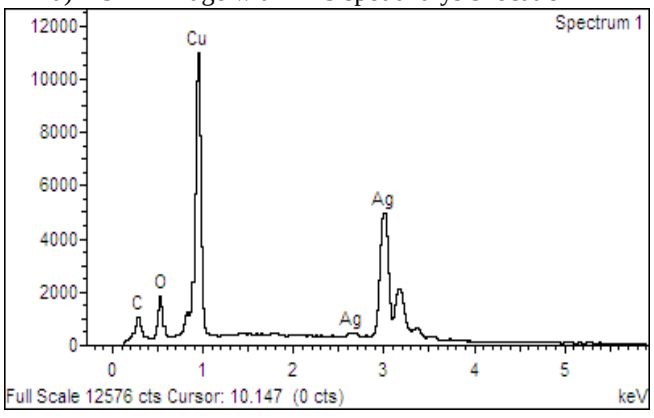

b) EDX spectrum of the corresponding spot in Fig 9a

Fig. 9: SEM images and corresponding EDX analysis of the fracture surfaces of nano-Ag sintered in ambient air.

Sintering nano-Ag in N_2 atmosphere reduced the Cu oxide formation and enhanced the sintering of the nano-Ag paste on the Cu substrate. This improvement in sintering conditions increased the shear strength to 10 MPa. Failure interface shifts to the die attach layer of the sintered nano-Ag joint and the back-metallization of the silicon dies, as shown in Fig. 10e and 10f. Plastic deformations such as elongated void were visible on the fracture surface of the sintered nano-Ag joint.

In the presence of N_2-5%H_2, the nano-Ag sintered joint produced the highest die shear strength of 17 MPa amongst the three sintering conditions. The results could be attributed to the ability to sinter on the H_2 reduced Cu substrate. This result is somewhat surprising when the DSC results only showed a broad endothermic peak and complete absence of an exothermic peak. However, cross-section of this nano-Ag joint, shown in Fig. 11, shows strong bonding to the Cu substrate. Furthermore, the fracture surfaces of the joints are also covered with sintered Ag flakes and void formation, as depicted in Fig. 10c and 10d.

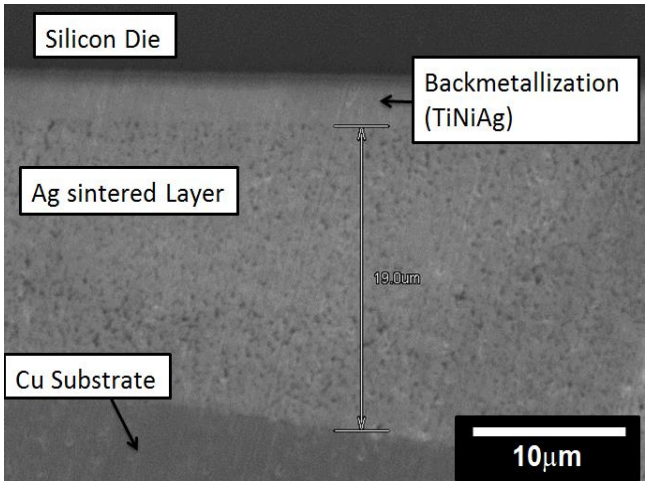

Fig. 11: Cross-section of nano-Ag sintered on Cu at N_2-5%H_2

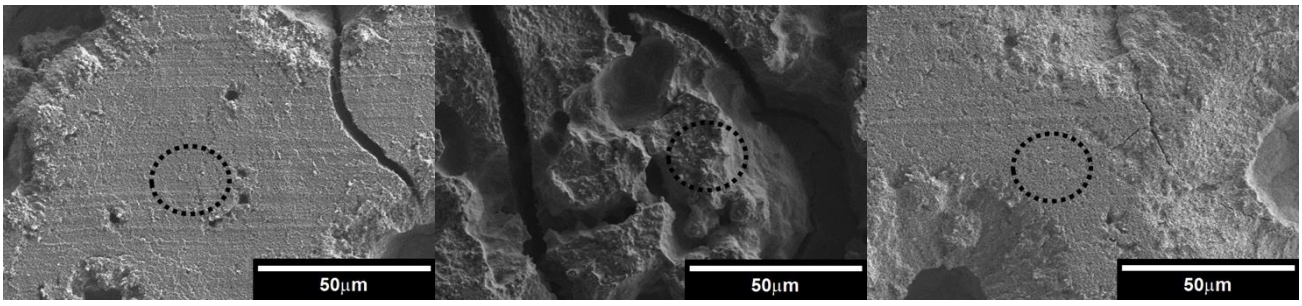

a) Air c) N_2-5%H_2 e) N_2

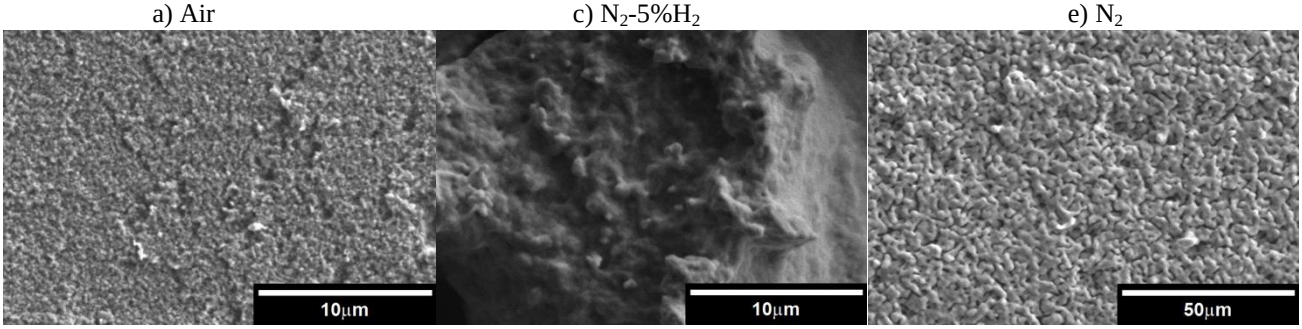

b) Air d) N_2-5%H_2 f) N_2

Fig. 10: Fracture surface of nano-Ag sintered on Cu substrate in different environment.

4. Conclusions

In this report, we presented the initial processing conditions for two pressureless silver pastes that can sinter on bare Cu substrate under different atmospheres. Based on the TGA and DSC analysis, peak temperatures of 230°C and 250°C were used to sinter the micron-Ag and nano-Ag pastes on the Cu substrate respectively. In the case of micron-Ag paste, the die shear strength exceeded 14 MPa when the oxygen from ambient air was able to oxidize the binders and reduce the Ag oxides to Ag to form bonding amongst the Ag flakes and between the Ag flakes and the Cu substrate. For nano-Ag paste, die shear strength of more 17 MPa, were obtained when sintering was conducted in N_2-5%H_2 environment. The presence of H_2 reduced any Cu oxide to allow good bonding between the Ag nanoparticles and Cu substrate. The fractured surfaces of these sintered Ag joints reflected the bonding strength at the sintering interfaces of Cu-Ag joints and the sintering kinetics of the Ag nanoparticles and micron-Ag flakes in the pastes.

Acknowledgments

We would like to acknowledge the support of UKM grant GGPM-2013-079 for this work.

References

[1] V. Chidambaram, J. Hattel, and J. Hald, "High-temperature lead-free solder alternatives," *Microelectron. Eng.*, vol. 88, pp. 981-989, 2011.

[2] V. R. Manikam and K. Y. Cheong, "Die attach materials for high temperature applications: a review," *IEEE Trans. Compon. Packag. Manuf. Tech.*, vol. 1, pp. 457-478, 2011.

[3] K. S. Siow, "Are sintered silver joints ready for use as interconnect material in microelectronic packaging? ," *J Electron. Mater.*, vol. 43, pp. 947-961, 2014.

[4] K. S. Siow, "Mechanical Properties of Nano-Ag as Die Attach Materials," *J. Alloys Compd.*, vol. 514, pp. 6-14, 2012.

[5] M. Knoerr and A. Schletz, "Power semiconductor joining through sintering of silver nanoparticles: evaluation of influence of parameters time, temperature and pressure on density, strength and reliability," in *Proc. 6th Int. Conf. Integr. Power Electron. Syst.*, 2010, pp. 1-6.

[6] C. Buttay, A. Masson, J. Li, M. Johnson, M. Lazar, C. Raynaud, *et al.*, "Die attach of power devices using silver sintering - Bonding process optimisation and characterization," in *Proceedings - 2011 IMAPS International Conference on High Temperature Electronics Network, HiTEN 2011*, Oxford, 2011, pp. 84-90.

[7] S. Joo and D. F. Baldwin, "Adhesion mechanisms of nanoparticle silver to substrate materials: identification," *Nanotech.*, vol. 21, pp. 055204-15, 2010.

[8] Y. Mei, G. Q. Lu, X. Chen, S. Luo, and D. Ibitayo, "Migration of sintered nanosilver die-attach material on alumina substrate between 250°C and 400°C in dry air," *IEEE Trans. Device Mater. Relia.*, vol. 11, pp. 316-322, 2011.

[9] G. I. N. Waterhouse, G. A. Bowmaker, and J. B. Metson, "The thermal decomposition of silver (I, III) oxide: A combined XRD, FT-IR and Raman spectroscopic study," *Phys. Chem. Chem. Phys.*, vol. 3, pp. 3838-3845, 2001.

[10] J. C. Brinker and G. W. Scherer, *The Physics and Chemistry of Sol-Gel Processing*. London: Academic Press Inc, 1990.

[11] H. Zheng, D. Berry, K. D. T. Ngo, and G. Q. Lu, "Chip-bonding on copper by pressureless sintering of nanosilver paste under controlled atmosphere," *IEEE Transactions on Components, Packaging and Manufacturing Technology*, vol. 4, pp. 377-384, 2014.

[12] E. Ide, S. Angata, A. Hirose, and K. F. Kobayashi, "Bonding of various metals using Ag metallo-organic nanoparticles - A novel bonding process using Ag metallo-organic nanoparticles," *Mater. Sci. Forum*, vol. 512, pp. 383-388, 10 November 2004 through 12 November 2004 2006.

[13] E. Ide, S. Angata, A. Hirose, and K. F. Kobayashi, "Metal-metal bonding process using Ag metallo-organic nanoparticles," *Acta Mater.*, vol. 53, pp. 2385-2393, 2005.